Published in final edited form as:

Cancer Res. 2018 March 01; 78(5): 1200–1213. doi:10.1158/0008-5472.CAN-17-2876.

Familial and Somatic *BAP1* Mutations Inactivate ASXL1/2-Mediated Allosteric Regulation of BAP1 Deubiquitinase by Targeting Multiple Independent Domains

Hongzhuang Peng[1], **Jeremy Prokop**[2], **Jayashree Karar**[1], **Kyewon Park**[1], **Li Cao**[3], **J. William Harbour**[4], **Anne M. Bowcock**[5], **S. Bruce Malkowicz**[6], **Mitchell Cheung**[7], **Joseph R. Testa**[7], and **Frank J. Rauscher 3rd**[1]

[1]Wistar Institute, Philadelphia, PA, USA

[2]HudsonAlpha Genome Sequencing Center, Huntsville AL, USA

[3]Washington University in St Louis, St. Louis, MO

[4]University of Miami School of Medicine, Miami, FL, USA

[5]Icahn School of Medicine at Mount Sinai, New York, NY

[6]University of Pennsylvania and Veterans Affairs Medical Center Philadelphia, Philadelphia PA, USA

[7]Fox Chase Cancer Center, Philadelphia, PA, USA

Abstract

Deleterious mutations of the ubiquitin carboxy-terminal hydrolase BAP1 found in cancers are predicted to encode inactive truncated proteins, suggesting that loss of enzyme function is a primary tumorigenic mechanism. However, many tumors exhibit missense mutations or in-frame deletions or insertions, often outside the functionally critical UCH domain in this tumor suppressor protein. Thus, precisely how these mutations inactivate BAP1 is unknown. Here, we show how these mutations affect BAP1 interactions with the Polycomb group-like protein ASXL2, using combinations of computational modeling technology, molecular biology, and in vitro reconstitution biochemistry. We found that the BAP1-ASXL2 interaction is direct and high affinity, occurring through the ASXH domain of ASXL2, an obligate partner for BAP1 enzymatic activity. The ASXH domain was the minimal domain for binding the BAP1 ULD domain, and mutations on the surfaces of predicted helices of ASXH abolished BAP1 association and stimulation of BAP1 enzymatic activity. The BAP1-UCH, BAP1-ULD, and ASXH domains formed a cooperative stable ternary complex required for deubiquitination. We defined four classes of alterations in BAP1 outside the UCH domain, each failing to productively recruit ASXH to the wild-type BAP1 catalytic site via the ULD, resulting in loss of BAP1 ubiquitin hydrolase activity. Our results indicate that many BAP1 mutations act allosterically to inhibit ASXH binding, thereby

Correspondence: Frank J. Rauscher, 3rd, Wistar Institute, 3601 Spruce Street, Philadelphia, PA 19104; Phone: 215-898-0995; Fax: 215-898-3929; rauscher@wistar.org; Joseph R. Testa, [5]Fox Chase Cancer Center, 333 Cottman Avenue, Philadelphia, PA; Phone: 215-728-2610; Fax: 215-214-1623; joseph.testa@fccc.edu.

Disclosure of Potential Conflicts of Interest

The authors declare no potential conflicts of interests specifically related to this work.

leading to loss of enzyme activity. Small molecule approaches to reactivate latent wild-type UCH activity of these mutants might be therapeutically viable.

Précis:

Combined computational and biochemical approaches demonstrate that the BAP1-ASXL2 interaction is direct and high affinity and that many *BAP1* mutations act allosterically to inhibit BAP1-ASXL2 binding.

Keywords

BAP1; PR-DUB; ASXL1/2; mutations; deubiquitinase; cancer; tumor susceptibility

Introduction

BAP1 was identified as a ubiquitin hydrolase that binds to the RING finger domain of BRCA1 and enhances BRCA1-mediated inhibition of breast cancer cell growth (1). The N-terminal 240 amino acids of BAP1 show significant homology to a class of thiol proteases, designated ubiquitin C-terminal hydrolases (UCH), one of several classes of deubiquitinating enzymes implicated in proteolytic processing of ubiquitin. BAP1 residues forming the catalytic site (Q85, C91, H169 and D184) are completely conserved. BAP1 contains two protein binding motifs for BRCA1 and BARD1 that form a tumor suppressor heterodimeric complex (2), as well as a binding domain for HCF1, which interacts with histone-modifying complexes during cell division (3). The C-terminus of BAP1 contains two nuclear localization signals and a UCH37-like domain (ULD). BAP1 interacts with ASXL family members to form the polycomb group repressive deubiquitinase complex involved in stem cell pluripotency and other developmental processes (4,5).

BAP1 is a nuclear-localized UCH that can cleave ubiquitin substrates *in vitro*. The UCH homology of BAP1 implies a role for either ubiquitin-mediated, proteasome-dependent degradation or other ubiquitin-mediated regulatory pathways in BRCA1 function (1,6). Regulated ubiquitination of proteins and subsequent proteasome-dependent proteolysis play a role in almost every cellular growth, differentiation and homeostatic process (6,7). The pathway is regulated by enzymes at the level of proteolytic deubiquitination and ubiquitin hydrolysis and are classified into two families: ubiquitin specific proteases (UBPs) and UCHs. The UBPs cleave ubiquitin or ubiquitin-conjugates from large substrates, whereas UCHs such as BAP1 cleave ubiquitin from ubiquitin-conjugated small substrates.

BAP1 exhibits tumor suppressor activity in cancer cells (1,2). Frequent somatic mutations/deletions of *BAP1* are found in metastasizing uveal melanomas (8), malignant mesothelioma (9,10), and other cancers (Figure 1A). Families with heritable mutations of *BAP1* were first published simultaneously in two papers in *Nature Genetics*; one reported two families with a high incidence of mesothelioma, uveal melanoma, and several types of epithelial cancer, such as renal carcinoma (10); the second reported two families with numerous cases of atypical melanocytic tumors and occasional uveal and cutaneous melanomas (11). Contemporaneously, a third group independently reported a family with a germline *BAP1*

mutation associated with uveal melanoma, lung adenocarcinoma, meningioma, and other cancers (12). Subsequently, numerous reports have expanded on the discovery of germline *BAP1* mutations in families with these and other cancers (13,14), now defined as the BAP1 tumor predisposition syndrome.

Mutations/deletions in *BAP1* cause premature protein termination, protein instability, and/or loss of UCH catalytic activity. Homozygous deletion of mouse *Bap1* is embryonic lethal, while systemic deletion in adults recapitulates features of human myelodysplastic syndrome (15). Heterozygous *Bap1* knockout and knock-in mice survive but develop numerous spontaneous malignant tumors and increased susceptibility to asbestos-induced mesothelioma formation (16). Knock-in mice expressing Bap1 revealed that BAP1 interacts with HCF1, OGT, and polycomb group proteins ASXL1 and ASXL2 *in vivo* (15).

BAP1 functions as part of a large polycomb-like complex that has an obligate partner for enzyme activity, the ASXL1/2 family members (5). *Drosophila* PcG Calypso protein is highly homologous to BAP1. Calypso complexes with the PcG protein Asx, and this Polycomb repressive deubiquitinase (PR-DUB) complex binds to PcG target genes. The human homologues of Asx are ASXL1/2/3 (Figure 1B). The N-terminus of ASXL, which contains the highly conserved ASXH domain (ASX homologous, AB boxes), is required for Calypso/BAP1 protein association. Similar to *Drosophila* Asx, human ASXL1/2 complexes with BAP1 to deubiquitinate H2A ub1 (5), thus providing evidence that an epigenetic modifier and associated proteins play a special role in modifying chromatin. However, the mechanism by which cancer-related mutations in *BAP1* and other PR-DUB genes and their encoded proteins/protein complexes has not been determined.

Mutations of *ASXL1/2/3* genes leading to protein truncations have been found to associate with human cancers and other diseases. *De novo* nonsense mutations in *ASXL1* cause Bohring-Opitz syndrome, a severe malformation disorder (17), and *de novo* truncating mutations in *ASXL3* result in a clinical phenotype with some similarities (18). Somatic mutations in *ASXL1* in patients with myeloid disorders/leukemias are associated with adverse outcome (19,20). ASXL1 is an epigenetic modifier that plays a role in polycomb repressive complex 2 (PRC2)-mediated transcriptional repression in hematopoietic cells, and ASXL1 loss-of-function mutants in myeloid malignancies result in loss of PRC2-mediated gene repression of leukemogenic target genes (19).

In this study, we define molecular mechanisms whereby tumor-derived, discrete in-frame deletions and insertions outside of the BAP1 catalytic domain perturb BAP1-ASXL2 interactions leading to tumor-related loss of BAP1 catalytic activity.

Materials and Methods

Plasmids

The pC3-BAP1-FL(6His), pC3-BAP1-FL,C91S(6His), pC3.1-Myc-BAP1, FL wild type (WT), and patient-related *BAP1* mutations/deletions [C91W, S172R, D672G, ΔE283-S285, ΔE631-A634, ΔK637-C638(sub of N), ΔR666-H669] plasmids were constructed through PCR-based cloning. The nucleotide locations for these mutations, corresponding to those

observed in uveal melanoma patients (8), are as follows: C91W(NT: T388G); S172R(NT: C631G); D672G(NT: A2130G); ΔE283-S285(NT: 960–968 del); ΔE631-A634(NT: 2006–2017 del); ΔK637-C638 sub of N(NT: 2026–2028 del); and ΔR666-H669(NT: 2112–2120 del). Note that the C91W mutation was originally reported as C91G (8), but was later corrected following discussions with staff affiliated with the COSMIC cancer database. The pEZ-M12-BAP1-WT and mutation/deletion plasmids were from AMB. The C91S mutation, originally described by Jensen et al. (1), is known to yield a protein with no detectable UCH activity. The pFastBacHTa-BAP1, FL WT, and mutations/deletions from patients [C91W, S172R, D672G, ΔE283-S285, ΔE631-A634, ΔK637-C638(sub of N), ΔR666-H669] constructs were sub-cloned from pC3.1-Myc-BAP1, FL WT, and mutations/deletions plasmids. The UCH-WT and UCH-C91S mutant plasmids were also sub-cloned (1). All plasmids were sequenced to confirm the authenticity of the *BAP1*-and *ASLX*-mutant inserts. Additionally, pGEX-4T-1-BAP1-FL was sub-cloned from pC3.1-Myc-BAP1 and FL-WT, and pGEX-2TK-BAP-UCH-WT (1–250 aa) was previously reported (1). The pGEX-4T-1-BAP1-ULD and pQE30-BAP1-ULD (601–729) plasmids were constructed through PCR-based cloning. Plasmids with the mutations pQE30-BAP1-ULD, L650P, or F660P were introduced using Quikchange site-directed mutagenesis (Stratagene). The pQE30-BAP1-ULD plasmids with mutations or deletions D72G, ΔE283-S285, ΔE631-A634, ΔK637-C638 (sub of N), or ΔR666-H669 were constructed via PCR-based cloning.

The fragments pC3.1-Flag-ASXL2 (261–1435aa), pC3.1-Flag-ASXL2 (261–649 aa), pQE30-ASXL2 (261–649aa), pFastBac-Flag-ASXL2 (261–1435 aa), pFastBac-Flag-ASXL2 (261–649 aa), pFastBacHTb-ASXL2 (261–1435 aa), pFastBacHTb-ASXL2 (261–649 aa) were sub-cloned from pBluescriptR-ASXL2 (Open Biosystem) into pC3.1-Flag, pQE30, and pFastBacHTb vectors, respectively. The pQE30-ASXL2-AB (261–381 aa), pQE30-ASXL2-A (261–318 aa), and pQE30-ASXL2-B (319–381 aa) plasmids were constructed through PCR-based cloning. The pQE30-ASXL2-AB mutations (R284P, VDR-AAA, NEF-AAA, ERL-AAA, EKE-AAA) were introduced by Quikchange site-directed mutagenesis (Stratagene).

Proteins expression and purification

The ^{35}S-labeled BAP1-FL, ASXL2 (261–1435 aa), and ASXL2 (261–469aa) probes were produced by coupled *in vitro* transcription and translation (IVT) using TNT@T7 quick coupled transcription/translation system (Promega).

The baculovirus (Bv) His-BAP1-FL WT and mutant proteins were expressed individually or co-expressed with Flag-ASXL2 (261–649 aa) protein in Bv-infected Sf9 cells (Wistar Protein Expression and Molecular Screening Facilities). High-titer Bv stocks for each protein were prepared using standard techniques, and Sf9 cells were infected for 48 h. The cells were harvested, and pellets were lysed for protein preparation or stored at −80°C.

The GST-and His-tagged BAP1 and ASXL2 proteins were expressed in *E. coli* BL21 (DE3) (Stratagene) and SG13009 (S9) (Qiagen), respectively. The bacteria bearing the desired plasmid were propagated with aeration at 37°C in 800 ml of 2YT to an A_{600} absorbance of approximately 0.6. IPTG was added to 1 mM, and growth was continued at either 37°C for 3 hours or 20°C overnight. The cells were then harvested by centrifugation.

The Bv-expressed proteins were purified using either ANTI-FLAG M2 Affinity Gel (Sigma) or Ni-NTA resin (Qiagen) as recommended by the manufacturers. The GST-fusion proteins were purified as described (21). The bacterial His-tagged proteins were purified under denaturing conditions (Qiagen) and re-folded by dialysis as described (21).

GST association assays

GST association assays were performed as described (22).

Ub-AMC Assay

Cleavage of Ub-AMC by wild type or BAP1 mutants or by co-expressed proteins, e.g., BAP1-ASXL2-AB (wild type and mutant forms) was assayed in reactions containing 5 nmol Ub-AMC and the indicated proteins or complexes. Ub-AMC activity was assayed at 25°C in 20 mM HEPES buffer (pH 7.5), 100 mM NaCl, 1 mM EDTA, 5 mM DTT, and 0.05% (w/v) Tween-20. Assays were performed in 384-well plates (PerkinElmer) in a 30 μl reaction volume. Fluorescence was measured at 5-min intervals at excitation and emission wavelengths of 355 nm and 460 nm, respectively. The release of AMC was monitored by fluorescence spectroscopy at 436 nm. All assays were performed simultaneously in duplicates. The hydrolysis rate was linear for 40~60 min and corrected for background signal (no enzyme).

Immunoprecipitation and Western blot analysis

For detecting IVT BAP1 and ASXL2 protein interactions, co-immunoprecipitation (co-IP) was performed by mixing IVT BAP1 and ASXL2 proteins in 1xPBS in 100 μl reaction volume at 37°C for 1 h. The co-IP was performed in RIPA buffer with 10 μg of BAP1 (rAb) at 4°C for 1 h, followed by adding Protein A/G plus-Agarose (Santa Cruz) and continued incubation for an additional 1 h. The resin was washed with RIPA buffer, then extracted with 5x Laemmli sample buffer. The protein complex was resolved in 4–12% NuPAGE (Invitrogen) in MOPS running buffer. The gel was then dried and exposed on X-ray film.

For detecting the interaction between BAP1-FL WT/mutant proteins and ASXL2 (261–649 aa) protein, IP-Western blotting was performed. These proteins were expressed from Bv and purified with either Ni-NTA resin (Qiagen) or ANTI-FLAG M2 Affinity Gel [anti-Flag (mAb)] (Sigma). The purified His-BAP-FL WT/mutant proteins were added to the resin, in which the Flag-ASXL2 protein was already bound in binding buffer (50 mM Tris-HCl, pH 7.4, 150 mM NaCl, 2 mM EDTA, 0.25% NP40, 2% BSA). The association reaction was incubated at RT for 1 h. The resin was washed with washing buffer [50 mM Tris-HCl, pH 7.4, 150 mM NaCl (500 mM NaCl for the last wash, desalted with 20 mM Tris-HCl), 5 mM EDTA, 0.5% NP40], and extracted with 5x Laemmli sample buffer. The protein complex was resolved in 4–12% NuPAGE (Invitrogen) in MES running buffer. Western blot analysis was performed using BAP1(rAb) (Rauscher laboratory) and Flag(rAb) (Cell Signaling) antibodies.

To detect the association of BAP1 WT/mutant proteins and ASXL2 (261–649 aa) protein *in vivo*, HEK 293 cells were co-transiently transfected with both plasmids expressing BAP1 WT/mutant and ASXL2 proteins (Lipofectamine 2000) (Invitrogen), as described (Peng JBC

2009). At 48 h post-transfection, cells were collected and whole cell lysates were used for co-IP with ANTI-FLAG M2 Affinity Gel [anti-Flag (mAb)] (Sigma). Western blot analyses were performed with BAP(rAb) and Flag(rAb) antibodies.

Gel filtration analysis

Gel filtration was carried out as described (23). The purified individual BAP1-UCH, BAP1-ULD, and ASXL2-AB proteins or preformed BAP1-UCH-ULD-AB protein complex were analyzed by gel filtration with a Superdex 200 HR 10/30 column (GE Healthcare) equilibrated in BB100 buffer (20 mM Tris-HCl, pH 8.0, 100 mM NaCl, 0.2 mM EDTA, 10% glycerol). The column was set at 4°C; the flow rate was 0.5 ml/min, and 1-ml fractions were collected. Sixty μl of the proteins or protein complex from each fraction were mixed with 5x Laemmli sample buffer, heated, and resolved on Nu-PAGE (Invitrogen). The proteins were visualized by Coomassie Blue stain.

Modeling of protein complex

The sequence of the UCH domain of human BAP1 (Q92560) was blasted against the Protein Data Bank (pdb), which revealed structure 3a7s (of UCH-L5/UCH37) as the most homologous. Amino acids were changed on 3a7s to those found in BAP1 and the larger loop of BAP1 built using homologous sequence/structures of pdb 2nxp and 3zzw. The structure was energy minimized multiple times using AMBER03 force field (24) in water using YASARA structure (25). This structure was aligned to each of the UCH domains of known protein structures for UCH-L1 (pdb 3kw5), UCH-L3 (pdb 2we6), and UCH-L5 (pdb 3ris) using MUSTANG algorithm (26). Sequences for ASXL were aligned from human ASXL1 (Uniprot Q8IXJ9), mouse ASXL1 (P59598), human ASXL2 (Q76L83), mouse ASXL2 (Q8BZ32) and *Drosophila melanogaster* ASX (Q9V727) using ClustalW2 (27), revealing a highly conserved domain (composed of box A and B). Structures for this domain were created using QUARK (28) *ab initio* modeling and energy minimized. Docking locations for ASXL were identified using overlapping 10-aa fragments of the ASXL model to the BAP1-UCH model using AutoDock (29), with 25 confirmation for each run. Using the top binding energies of all docking experiments, the full ASXL model was aligned to BAP1-UCH domain and interactions energy minimized. Models for BAP1-ULD were created using QUARK, selecting for optimal hydrophobic packing, and aligned to the structure of BAP1-UCH using pdb 3ihr (UCH-L5 with its ULD domain) with the MUSTANG algorithm.

Results

Structure analysis for BAP1, ASXL1/2/3, and mutations/deletions/truncations in cancer patients and other human diseases

The domain structure of BAP1 is unique (Figure 1A). The UCH domain is similar to other mammalian UCHs (UCH-L1, UCH-L3, and UCH-L5). Mutations in the conserved catalytic site residues (Q85, C91, H169, and D184) completely abolish BAP1 ubiquitin hydrolase activity. Mutations C91W and H169Q in the catalytic site of UCH were identified in uveal melanomas (8). Other mutations/deletions/truncations in BAP1-UCH were found in uveal melanomas, mesothelioma and breast cancer, and were confirmed as loss-of-function changes leading to loss of enzymatic activity (30). BAP1 interacts with BARD1 and BRCA1

and inhibits the E3 ligase activity of BRCA1/BARD1. Therefore, BAP1 has been proposed to regulate BRCA/BARD1-mediated ubiquitination during DNA damage response and cell cycling (2). The consensus sequence NHNY of BAP1 is critical for its interaction with HCF1, a transcriptional cofactor found in regulatory complexes. BAP1 mediates HCF1 deubiquitination and thereby helps control cell proliferation by regulating HCF1 protein levels and by associating with genes involved in cell cycle regulation (3). The C-terminus ULD domain associates with the RING finger of BRCA1 involved in forming the BRCA1/BARD1 heterodimer, and this complex coordinately regulates ubiquitination during DNA damage response and cell cycling (1,2). The ULD domain also interacts with ASXL members to form the PR-DUB involved in stem cell pluripotency and developmental processes (5). Many mutations/deletions/truncations in the ULD domain were identified in human cancers (8,10) (Figure 1A). However, the molecular mechanism for these alterations remains elusive.

ASXL1/2/3 are human homologues of *Drosophila* Asx (Figure 1B). These Asx family members share many similar domain structures. The N-terminus of ASXL contains a highly conserved ASXH domain, composed of the AB box required for Calypso/BAP1 protein binding. The C-terminus has a highly conserved plant homeo domain (PHD). The associated proteins for the PHD of the Asx family remain unknown. Several mutations in ASXL proteins have been found in myeloid leukemia and other disorders. However, the mechanism by which such mutations cause cancer and other diseases remains unclear.

We investigated the molecular mechanism for the mutations/deletions occurring in either the N-terminus of UCH or in the C-terminus of ULD domain for inactivating BAP1 in cancer, as well as for mutations occurring in ASXL proteins (Figure 1A, 1B). ASXL functions as a molecular scaffold to recruit BAP1 to transcription factors, such as YY1, which specifically bind to its target genes. The N-terminus of ASXL, which includes ASXH, binds the ULD domain of BAP1, allowing the UCH catalytic site to be brought in proximity to the target promoter. ASXL then associates with transcription factors that bind to its target promoter. BAP1 ubiquitin hydrolase specifically removes ubiquitin from histones of chromatins, thereby repressing target genes. Our hypothesis is that BAP1-UCH, BAP1-ULD and ASXL-AB tripartite binding is required for enzyme activity and for deubiquitination of histone H2A. Thus, in this model, BAP1 and associated epigenetic modifiers (complexes) play a specific role in modifying chromatin and regulating gene transcription. To test this hypothesis and to explain how mutations/deletions/truncations occurring in either ULD or UCH domains inactivate BAP1 in cancer, we used computer predicted molecular modeling of these proteins as a guide and biochemically characterized the protein-protein and/or domain-domain interactions of BAP1 and ASXL2 *in vivo* and *in vitro* using highly purified recombinant proteins, in coordination with BAP1 ubiquitin enzymatic activity.

Direct interaction between BAP1 and ASXL2

Association of BAP1 with ASXL2 was tested *in vitro* by binding of full-length BAP1 to ASXL2. Immunoprecipitation (IP) was performed for both ^{35}S-labeled BAP1 and ASXL2 using BAP1 (rAb). BAP1 was bound to ASXL2 (261–1435 aa) and ASXL2 (261–649 aa)

(Figure 2A). The N-terminal region of ASXL2 (261–649 aa), containing the predicted AB box, is necessary and sufficient for interaction with BAP1.

We next wanted to recapitulate the association between BAP1 and ASXL2 using recombinant proteins. BAP1 and ASXL2 proteins were produced in Bv by single-or co-expression. Single-expressed BAP1 WT, C91S mutant, and ASXL2 proteins were soluble and easily affinity-purified either with Ni-NTA or ANTI-FLAG M2 Affinity Gels (Figure 2B). ASXL2 could be readily pulled down by either BAP1 WT or C91S proteins, based on Ni-NTA resin purification of co-expressed recombinant His-tagged proteins.

ASXL2 stimulates BAP1 ubiquitin hydrolase activity

Since BAP1 associates with ASXL2 *in vitro* and *in vivo*, BAP1 ubiquitin hydrolase activity was tested using purified recombinant proteins produced from Bv. Ub-AMC was used as substrate for the BAP1 enzymatic assay. BAP1 WT protein alone showed UCH basal deubiquitinase activity, whereas ASXL alone did not (Figure 2C). When both proteins were mixed, ASXL2 greatly stimulated WT BAP1 activity, whereas a BAP1 mutant affecting the active cysteine (C91S) was enzymatically inactive (Figure 2C), indicating that ASXL2 not only binds to BAP1 but also stimulates its ubiquitin hydrolase activity.

The AB box of ASXL2 is the minimal domain for interaction with BAP1 and stimulation of BAP1 ubiquitin hydrolase activity

To define the minimal domain of ASXL2 required to interact with BAP1, we made truncations of ASXL2 based on computer predictions of homologous domains having stable structure fold predictions (Figure 3A). Truncated proteins were expressed and purified from Bv and *E. coli* (Bac), followed by analysis for BAP1 binding (Figure 3B, *left*). ASXL2 (261–649 aa) and AB box proteins were pulled down by GST-BAP1, while A box or B box of ASXL2 was not adequate to bind BAP1 (Figure 3B, *right*). As shown by the negative control, ASXL2 (261–649 aa) did not bind GST. Next, we asked whether the AB box of ASXL2 stimulates BAP1 ubiquitin hydrolase activity as well as ASXL2 (261–649 aa). Ub-AMC assays were performed for BAP1 WT protein and truncated ASXL2 proteins. BAP1 showed basal ubiquitin hydrolase activity (Figure 3C). The AB box of ASXL2 significantly stimulated BAP1 activity, as did ASXL2 (261–649 aa), whereas box A or B alone had intermediately stimulatory effects on BAP1 activity (Figure 3C). These data suggest that the predicted AB box of ASXL2 is the minimal domain for binding to BAP1 and stimulating its ubiquitin hydrolase activity, and are also consistent with BAP1's association with ASXL1 (2–365 aa) (5).

To define potential protein-protein interaction surfaces between BAP1 and ASXL2-AB, we investigated amino acid alignments of ASXH AB boxes of ASXL members from human, mouse, and *Drosophila*. Conserved amino acids were visualized on a predicted molecular model of the ASXH domain (Figure 4A, 4B, cyan), which revealed several potential interaction sites. The AB box is predicted to form five helices. The amino acid residues are very conserved in the AB box among ASXL members for hydrophobic packing of the domain (Figure 4B, cyan). As confirmed through AutoDock experiments, several conserved surface amino acids were suggested to be critical to binding of the ASXH domain to BAP1

(Figure 4B, middle structures, red). We suspected that these conserved amino acids of the AB box are important for direct interaction with BAP1. We made mutations for these amino acids by either disrupting the helix structure (R284P in Helix 1) or by changing conserved amino acids to alanines on surfaces of helices (VDR-AAA, NEF-AAA, ERL-AAA, EKE-AAA in Helices 2, 3 and 4, respectively) (Figure 4A, B). All WT and mutant AB box proteins were produced in Bac and purified (Figure 4C, *left*). GST-BAP1 association assays with WT and mutant AB box proteins were performed. As expected, WT AB Box was pulled down by GST-BAP1 protein (Figure 4C, *right*). Mutant AB box proteins (R284P: Helix 1; EKE-AAA: Helix 4) had intermediate effects on BAP1 binding, whereas VDR-AAA, NEF-AAA, and ERL-AAA (located in Helices 2 and 3) caused marked defects in BAP1 binding (Figure 4C, *right*), suggesting these conserved amino acids in helices of the AB box make direct contact with BAP1 and that mutations of these amino acids disrupt its interaction with BAP1. This suggests that Helices 2 and 3 of the AB box of ASXL2 are the major contacted surfaces toward BAP1.

We next investigated if AB box mutants with impact for BAP1 binding also coordinately lost stimulation of BAP1 ubiquitin hydrolase activity. Ub-AMC assays for BAP1 with AB box WT and mutant proteins were performed. As expected, BAP1 showed basal deubiquitin enzymatic activity and WT AB box stimulated BAP1 enzymatic activity (Figure 4D). However, mutations (VDR-AAA) and (NEF-AAA) of the AB box that failed to bind BAP1 coordinately lost the ability to stimulate BAP1 activity (Figure 4C, D). Furthermore, mutations (R284P), (ERL-AAA), and (EKE-AAA) that decreased binding to BAP1 showed less stimulation of BAP1 enzymatic activity as compared to WT AB box (Figure 4D). These data indicate that ASXL2 stimulation of BAP1 ubiquitin hydrolase activity coordinates well with interactions between ASXL2 and BAP1 and that stimulation of BAP1 activity requires physical association of ASXL2 with BAP1.

Cancer-derived alterations in the BAP1-ULD domain abolish ASXL2 association and stimulation activity

To investigate how cancer-related mutations/deletions of *BAP1* affect ASXL2 binding and BAP1 ubiquitin hydrolase activity, WT and mutant BAP1 proteins were produced in Bv and purified for ASXL2 binding *in vitro*. Bv Flag-ASXL2 (261–649 aa) was first bound to Flag (mAb) resin, and then purified WT and mutant BAP1 proteins were incubated with resin-bound ASXL2. Immunoblotting was performed for associated WT and mutant BAP1. BAP1 mutant S172R and BAP1 ΔE631-A634, ΔK637-C638, ΔR666-H669 significant abolished ASXL2 protein binding *in vitro* (Figure 5A, B; Supplemental Figure 1), indicating that BAP1 harboring in-frame deletions in the ULD domain abolished ASXL binding. In parallel, Ub-AMC assays were performed with ASXL2 and BAP1 WT and mutant proteins. Three different protein concentrations (1X, 2X, 4X) of BAP1 were mixed with ASXL2. ASXL2 greatly stimulated WT BAP1 activity in a dose dependent manner (Figure 5C). Although the catalytically dead BAP1 mutant C91W could bind to ASXL2, it showed no enzymatic activity. When present at low concentrations (1X, 2X), mutants with deletions in BAP1-ULD showed no or extremely low activity in the presence of ASXL2. At a high concentration (4X) of BAP1 deletion mutants, bound ASXL2 inhibited BAP1 E283-S285 activity. Although ASXL2 showed significantly decreased binding to BAP1 E631-A634, it

slightly inhibited BAP1 activity. BAP1 mutant K637-C638 showed no enzymatic activity in the presence of ASXL2, consistent with data demonstrating that the protein-protein interaction is lost between ASXL2 and BAP1 ΔK637-C638 (Figure 5A–C). Another BAP1 deletion, R666-H669, showed no binding to ASXL2 and, as expected, BAP1 activity was not affected by the presence of ASXL2, although the BAP1 deletion mutant R666-H669 itself showed some basal activity (Figure 5).

BAP-UCH, ULD and ASXL2-AB domains form a ternary stable complex *in vitro*

Structure predictions for BAP1-UCH suggest similar folding (Figure 6A) as compared to other UCH proteins whose structures have been solved; however, BAP1 contains a larger loop than the others. This suggests that larger substrates should be accessible to the catalytic cleavage site of BAP1, but the large loop is also likely to restrict the access site for ubiquitin. The ULD domain has been shown in UCH-L5 to interact with UCH (31), in which BAP1 also contains a highly homologous ULD. The ULD for BAP1 was thus modeled (Figure 6B) and amino acids in this domain associated with cancer were visualized (Figure 6B, yellow). Aligning the ULD and UCH domains of BAP1 to the structure of UCH-L5 (pdb 3ihr), allows for an approximation of the ULD interaction with UCH (Figure 6C, 6D). Docking of the ASXH domain to this structure suggests a tripartite consisting of a BAP1-UCH, BAP1-ULD, and ASXH domain complex. We predicted that the BAP1-ULD domain folds back on the UCH domain, and then the ULD domain recruits the ASXH domain, which subsequently stabilizes the UCH domain loop, thereby increasing catalytic activity of BAP1-UCH by opening the site of binding for histones and ubiquitin (Figure 6C, D). To prove this and reconstitute the tripartite protein complex *in vitro,* a GST-ULD association assay with ASXL2-AB protein was performed using highly purified recombinant proteins. ASXL2-AB protein was pulled down by GST-ULD protein, and this interaction between ULD and AB was found to be direct and specific (Figure 7A). Furthermore, GST-UCH also binds ULD, through which the ASXL2-AB box is recruited to GST-UCH. However, GST-UCH itself did not directly associate with ASXL2-AB (Figure 7B). To test whether UCH, ULD, and AB form a ternary stable complex, the purified proteins were mixed to pre-form a complex in solution, then subjected to gel filtration. Meanwhile, each individual purified protein was also subjected to gel filtration. As shown in Supplemental Figure 2 (Panel I), the protein complex containing UCH, ULD and AB was co-eluted. The peak fraction of the complex was eluted with apparent molecular mass of 44 KDa. Individual UCH, ULD, and AB proteins eluted more likely as monomers with expected molecular masses (Supplemental Figure 2, Panels II, III, and IV). The peak fraction of the AB box in the complex shifted dramatically from #17 to #15 compared to AB alone, supporting our hypothesis that BAP1-UCH, BAP1-ULD and ASXL2-AB form a ternary stable complex *in vitro* and that ULD recruits ASXL2-AB to access the BAP1-UCH catalytic motif. This complex is sustained during gel filtration.

According to molecular modeling shown in Figure 6C, BAP1-ULD is predicted to be composed of helices and associated with the ASXL2-AB box. The long helix of ULD is packed close to the UCH. We hypothesize that if this helix were disrupted, it would change the ULD such that its association with AB box and/or UCH domain would be affected. To test this hypothesis, two mutations (L650P, F660P) located in the middle of the long helix

were individually introduced into the ULD motif. Then, GST-UCH association assays were performed using highly purified WT and mutant ULD proteins and ASXL2-AB. Surprisingly, L650P and F660P mutants did not affect UCH binding; however, they did abolish AB box binding (Supplemental Figure 3), suggesting that the interface of the AB box is on the long helix of ULD and that disruption of this helix disassociates binding to the AB box.

We next investigated mutation/deletions affecting BAP1 ULD identical to those observed in cancer patients. These mutation/deletions are predicted to encode BAP1 ULD alterations located on the interfaces either to ASXL-AB or to UCH, thus affecting BAP1 ubiquitin hydrolase activity (Figure 6C). Therefore, GST-UCH association assays were carried out with purified BAP1 ULD WT and mutant proteins and ASXL2-AB. Mutation/deletions in BAP1 ULD impacted UCH and/or AB box binding (Figure 7C). BAP1 ULD mutants D672G and K637-C638 slightly decreased UCH binding but significantly decreased AB box association. However, BAP1 ULD mutants E631-A634 and R666-H669 significantly decreased UCH binding and almost completely abolished AB box binding (Figure 7C), consistent with *in vitro* binding of full-length BAP1 with ASXL2 (261–649 aa) shown in Figure 5A, 5B.

Discussion

Herein, we have characterized protein-protein interactions of BAP1 and ASXL2 using computer modeling, biochemical approaches, and enzymatic activity analyses. We also investigated the molecular mechanism underlying loss-of-function mutations/deletions affecting BAP1 and the BAP1-ASXL2 complex that contribute to tumor susceptibility and progression in patients with mesothelioma, uveal melanoma, and other cancers. We have drawn the following conclusions from our data. First, the interaction between BAP1 and ASXL2 is direct, and the association of ASXL2 greatly stimulates BAP1 hydrolase activity. Second, the highly conserved AB box of ASXL2 is the minimal domain required for the interaction with BAP1 and its stimulation of BAP1 ubiquitin hydrolase activity. Mutations/deletions of highly conserved amino acids in predicted helices within the AB box abolish its association with BAP1 and its ability to enhance BAP1 enzymatic activity. These conserved amino acids are predicted to be on the surface of helices in the AB box of ASXL2. Third, cancer-derived mutations/deletions in the BAP1-ULD abolish ASXL2 binding and thereby result in loss of ASXL2's ability to stimulate BAP1 activity. These alterations in BAP1-ULD are reside at protein-protein interfaces among the BAP1-ULD, BAP1-UCH, and ASXL-AB. Lastly, BAP1-UCH, BAP1-ULD and ASXL-AB could be reconstituted to from a ternary stable complex *in vitro* using recombinant proteins. The mutations structurally disrupted the predicted helix of the ULD domain of BAP1 and abolished ASXL2 binding. Alterations in the ULD domain of BAP1 occurring in cancers failed to recruit the ASXL2-AB box to the UCH catalytic site, such that BAP1 deubiquitin hydrolase activity was dramatically reduced.

A previous study defined interaction domains between *Drosophila* Calypso and Asx (2–337 aa) and between human BAP1 and ASXL1 (2–365 aa) (5). Here, we took advantage of molecular modeling for BAP1 and ASXL members. We predicted structures for these proteins based on known NMR and/or crystallization of proteins from evolutionarily highly

conserved homologous sequences/structures and computer simulation. We then further defined the structure for these conserved domains and docked the locations for protein-protein interaction of the complex. We defined the highly conserved AB box for the ASXL family and predicted its three-dimensional structure, which is composed of five helices bundling to form a stable conformation (Figure 4A, B). Our data implicate the AB box as the minimal domain required to interact with BAP1. The AB box also stimulates BAP1 deubiquitin activity (Figure 3A–C). Moreover, conserved amino acids on the surface of helices within the AB box directly interact with BAP1 (Figure 4A, B), and mutations of these amino acids impacted BAP1 binding and ubiquitin hydrolase activity (Figure 4C, D).

The structure predictions for BAP1-UCH suggest folding similar to that of other UCH proteins (Figure 6A). However, BAP1 contains a larger loop than the others, suggesting that larger substrates would be accessible to the catalytic cleavage site, such as ubiquitin. The ULD domain of UCH-L5 interacts with the UCH domain (31), and BAP1 contains a highly homologous ULD domain. Thus, the ULD for BAP1 was modeled (Figure 6B). Alignment of UCH and ULD of BAP1 to the structure of UCH-L5 allows for an approximation of the ULD interaction with the UCH of BAP1 (Figure 6C). Docking of the AB box to this structure revealed a tripartite BAP1-UCH, BAP1-ULD, and ASXL2-AB domain complex. We predicted that BAP1-ULD folds back to the UCH and that the ULD recruits the AB box, which subsequently stabilizes the UCH loop, thereby increasing the catalytic activity of BAP1-UCH (Figure 6C, D). Indeed, this tripartite complex was reconstructed *in vitro* using purified recombinant proteins (Figure 7A, B; Supplemental Figure 2). This experimental evidence supported the predicted molecular modeling for the protein complex. Surprisingly, BAP1 mutations L650P and F660P, within the long helix of ULD (Figure 6A–C), did not interfere with UCH binding, but did abolish association with the AB box. Both mutations (L650P, F660P) were predicted to kink the long helix of ULD and disrupt UCH binding. The interpretation is that either the AB box directly interacts with the long helix of ULD, or that the ULD conformation changes such that the AB box can no longer bind to ULD (Figure 6C, D; Supplemental Figure 3). Furthermore, we discovered a novel loss-of-function mechanism by which *BAP1* mutations/deletions occur in cancer. These mutations/deletions affect the interface of BAP1 with either ASXL-AB or UCH. Mutations of BAP1 ULD impact either AB box binding and/or UCH interactions. The tripartite complex stability is thereby adversely affected and UCH activity is markedly decreased, potentially altering BAP1's tumor suppressive activity. Deubiquitination of target proteins/chromatins by BAP1 are inhibited, resulting in derepression of target genes (Figure 7D). Our data provide evidence supporting the computer-predicted molecular modeling of the BAP1-ASXL interaction. The critical target proteins/chromatins for BAP1-ASXL2 repression remain to be determined. However, previous work suggests that ASXL proteins contain domains that likely serve in the recruitment of chromatin modulators and transcriptional effectors to DNA (32). ASXL1 plays a significant role in epigenetic regulation of gene expression by facilitating PRC2-mediated transcriptional repression of known leukemic oncogenes. Therefore, ASXL1 may serve as a scaffold for recruitment of the PRC2 complex to specific loci in hematopoietic cells, although ASXL loss leads to BAP1-independent alterations in chromatin state/gene expression in hematopoietic cells.

Based on our studies, we propose a working model for the mechanism of germline and/or somatic loss of BAP1 that increases susceptibility to various cancers. One scenario is that ASXL functions as a molecular scaffold to recruit BAP1 to transcription factors, which specifically bind to its target genes. Then, BAP1 ubiquitin hydrolase specifically removes the ubiquitin from histones of chromatins to repress these target genes (Figure 7D). ASXL not only functions as a molecular scaffold for BAP1 but also greatly stimulates its activity. When mutations/deletions occur in BAP1, either they cause enzymatic loss-of-function of BAP1 or abolish BAP1's association with ASXL. Loss of binding to ASXL would dramatically decrease BAP1 deubiquitination activity, because of inability to bring ASXL to BAP1's catalytic site (e.g., deletions in the ULD domain: E631-A634 del and K637-C638 del). On the other hand, products of *ASXL* gene mutations that lose association with BAP1 also lead to BAP1 loss-of-function. These mutations occur in highly conserved amino acids of the ASXL-AB box, the minimal domain required for BAP1 interaction. Thus, BAP1 ubiquitin hydrolase activity would be greatly reduced. Our study also suggests that ASXL loss would lead to BAP1-dependent alterations in chromatin state/gene expression in human cancers/disorders.

In summary, through an integrated use of advanced computational molecular modeling, molecular biology, and biochemistry strategies, we have provided evidence for a direct protein-protein interaction involving BAP1 and its physically obligate partner ASXL2 for ubiquitin hydrolase activity. We have also elucidated a molecular mechanism for certain naturally occurring loss-of-function *BAP1* mutations/deletions in cancer. *Drosophila* Calypso-Asx and human BAP1-ASXL2 complexes deubiquitinate H2A ub1, and mutations in chromatin modifying enzymes such as BAP1 are implicated in the epigenetic deregulation that occurs commonly in human cancers (5). It will be important to use epigenomic platforms to elucidate how these disease alleles contribute to tumorigenesis in different contexts. Moreover, many known oncogenes/tumor suppressors contribute, at least in part, to transformation through direct or indirect alterations in the epigenetic state (33). Further epigenomic studies of human malignancies will likely uncover novel routes to malignant transformation, and therapeutic strategies that reverse epigenetic changes might be of benefit in patients with mutations in epigenetic regulators.

Supplementary Material

Refer to Web version on PubMed Central for supplementary material.

Grant Support

This work was supported by NCI grants R01CA175691 (J.R. Testa, F.J. Rauscher), P30CA010815 (F.J. Rauscher), P30CA006927 (Fox Chase Cancer Center), R01CA161870 (J.W. Harbour, A.M. Bowcock), and R01CA163761 (F.J. Rauscher). Support for Shared Resources was provided by P30CA010815 to The Wistar Institute. Also supported by the Jayne Koskinas/Ted Giovanis Foundation for Health and Policy, a Maryland private foundation dedicated to effecting change in the health care industry for the greater public good (F.J. Rauscher), the Palmira and James Nicolo Family Research Fund (S.B. Malkowicz), Local #14 Mesothelioma Fund of the International Association of Heat and Frost Insulators & Allied Workers (J.R. Testa), Ovarian Cancer Research Fund Alliance (F.J. Rauscher), Samuel Waxman Cancer Research Foundation (F.J. Rauscher), a Susan G. Komen grant KG110708 (F.J. Rauscher), Office of the Assistant Secretary of Defense for Health Affairs, through the Breast Cancer Research Program, under Award Nos. W81XWH-17–1-0506, W81XWH-14–1-0235 and W81XWH-11–1-0494 (F.J. Rauscher). The opinions, findings, conclusions or recommendations expressed in this work are those of the authors and not necessarily of the directors, officers, or staff of the funding agencies listed here.

References

1. Jensen DE, Proctor M, Marquis ST, Gardner HP, Ha SI, Chodosh LA, et al. BAP1: a novel ubiquitin hydrolase which binds to the BRCA1 RING finger and enhances BRCA1-mediated cell growth suppression. Oncogene 1998;16:1097–112. [PubMed: 9528852]
2. Nishikawa H, Wu W, Koike A, Kojima R, Gomi H, Fukuda M, et al. BRCA1-associated protein 1 interferes with BRCA1/BARD1 RING heterodimer activity. Cancer Res 2009;69:111–9. [PubMed: 19117993]
3. Misaghi S, Ottosen S, Izrael-Tomasevic A, Arnott D, Lamkanfi M, Lee J, et al. Association of C-terminal ubiquitin hydrolase BRCA1-associated protein 1 with cell cycle regulator host cell factor 1. Mol Cell Biol 2009;29:2181–92. [PubMed: 19188440]
4. Gaytán de Ayala Alonso A, Gutiérrez L, Fritsch C, Papp B, Beuchle D, Müller J A genetic screen identifies novel polycomb group genes in Drosophila. Genetics 2007;176:2099–108. [PubMed: 17717194]
5. Scheuermann JC, de Ayala Alonso AG, Oktaba K, Ly-Hartig N, McGinty RK, Fraterman S, et al. Histone H2A deubiquitinase activity of the Polycomb repressive complex PR-DUB. Nature 2010;465:243–7. [PubMed: 20436459]
6. Isaksson A, Musti AM, Bohmann D. Ubiquitin in signal transduction and cell transformation. Biochim Biophys Acta 1996;1288:F21–9. [PubMed: 8764838]
7. Inobe T, Matouschek A. Paradigms of protein degradation by the proteasome. Curr Opin Struct Biol 2014;24:156–64. [PubMed: 24632559]
8. Harbour JW, Onken MD, Roberson ED, Duan S, Cao L, Worley LA, et al. Frequent mutation of BAP1 in metastasizing uveal melanomas. Science 2010;330:1410–3. [PubMed: 21051595]
9. Bott M, Brevet M, Taylor BS, Shimizu S, Ito T, Wang L, et al. The nuclear deubiquitinase BAP1 is commonly inactivated by somatic mutations and 3p21.1 losses in malignant pleural mesothelioma. Nat Genet 2011;43:668–72. [PubMed: 21642991]
10. Testa JR, Cheung M, Pei J, Below JE, Tan Y, Sementino E, et al. Germline BAP1 mutations predispose to malignant mesothelioma. Nat Genet 2011;43:1022–5. [PubMed: 21874000]
11. Wiesner T, Obenauf AC, Murali R, Fried I, Griewank KG, Ulz P, et al. Germline mutations in BAP1 predispose to melanocytic tumors. Nat Genet 2011;43:1018–21. [PubMed: 21874003]
12. Abdel-Rahman MH, Pilarski R, Cebulla CM, Massengill JB, Christopher BN, Boru G, et al. Germline BAP1 mutation predisposes to uveal melanoma, lung adenocarcinoma, meningioma, and other cancers. J Med Genet 2011;48:856–9. [PubMed: 21941004]
13. Carbone M, Yang H, Pass HI, Krausz T, Testa JR, Gaudino G. BAP1 and cancer. Nat Rev Cancer 2013;13:153–9. [PubMed: 23550303]
14. Pilarski R, Rai K, Cebulla C, Abdel-Rahman M. BAP1 tumor predisposition syndrome In: Adam MP, Ardinger HH, Pagon RA, Wallace SE, Bean LJH, Mefford HC, et al., editors. GeneReviews(R) Seattle (WA)1993.
15. Dey A, Seshasayee D, Noubade R, French DM, Liu J, Chaurushiya MS, et al. Loss of the tumor suppressor BAP1 causes myeloid transformation. Science 2012;337:1541–6. [PubMed: 22878500]
16. Kadariya Y, Cheung M, Xu J, Pei J, Sementino E, Menges CW, et al. Bap1 is a bona fide tumor suppressor: genetic evidence from mouse models carrying heterozygous germline Bap1 mutations. Cancer Res 2016;76:2836–44. [PubMed: 26896281]
17. Hoischen A, van Bon BW, Rodriguez-Santiago B, Gilissen C, Vissers LE, de Vries P, et al. De novo nonsense mutations in ASXL1 cause Bohring-Opitz syndrome. Nat Genet 2011;43:729–31. [PubMed: 21706002]
18. Bainbridge MN, Hu H, Muzny DM, Musante L, Lupski JR, Graham BH, et al. De novo truncating mutations in ASXL3 are associated with a novel clinical phenotype with similarities to Bohring-Opitz syndrome. Genome Med 2013;5:11. [PubMed: 23383720]
19. Abdel-Wahab O, Adli M, LaFave LM, Gao J, Hricik T, Shih AH, et al. ASXL1 mutations promote myeloid transformation through loss of PRC2-mediated gene repression. Cancer Cell 2012;22:180–93. [PubMed: 22897849]
20. Alvarez Argote J, Dasanu CA. ASXL1 mutations in myeloid neoplasms: pathogenetic considerations, impact on clinical outcomes and survival. Curr Med Res Opin 2017:1–7.

21. Peng H, Gibson LC, Capili AD, Borden KL, Osborne MJ, Harper SL, et al. The structurally disordered KRAB repression domain is incorporated into a protease resistant core upon binding to KAP-1-RBCC domain. J Mol Biol 2007;370:269–89. [PubMed: 17512541]
22. Peng H, Begg GE, Harper SL, Friedman JR, Speicher DW, Rauscher FJ, 3rd., Biochemical analysis of the Kruppel-associated box (KRAB) transcriptional repression domain. J Biol Chem 2000;275:18000–10. [PubMed: 10748030]
23. Peng H, Ivanov AV, Oh HJ, Lau YF, Rauscher FJ, 3rd., Epigenetic gene silencing by the SRY protein is mediated by a KRAB-O protein that recruits the KAP1 co-repressor machinery. J Biol Chem 2009;284:35670–80. [PubMed: 19850934]
24. Duan Y, Wu C, Chowdhury S, Lee MC, Xiong G, Zhang W, et al. A point-charge force field for molecular mechanics simulations of proteins based on condensed-phase quantum mechanical calculations. J Comput Chem 2003;24:1999–2012. [PubMed: 14531054]
25. Krieger E, Darden T, Nabuurs SB, Finkelstein A, Vriend G. Making optimal use of empirical energy functions: force-field parameterization in crystal space. Proteins 2004;57:678–83. [PubMed: 15390263]
26. Konagurthu AS, Whisstock JC, Stuckey PJ, Lesk AM. MUSTANG: a multiple structural alignment algorithm. Proteins 2006;64:559–74. [PubMed: 16736488]
27. Larkin MA, Blackshields G, Brown NP, Chenna R, McGettigan PA, McWilliam H, et al. Clustal W and Clustal X version 2.0. Bioinformatics 2007;23:2947–8. [PubMed: 17846036]
28. Xu D, Zhang Y. Ab initio protein structure assembly using continuous structure fragments and optimized knowledge-based force field. Proteins 2012;80:1715–35. [PubMed: 22411565]
29. Morris GM, Huey R, Lindstrom W, Sanner MF, Belew RK, Goodsell DS, et al. AutoDock4 and AutoDockTools4: Automated docking with selective receptor flexibility. J Comput Chem 2009;30:2785–91. [PubMed: 19399780]
30. Ohar JA, Cheung M, Talarchek J, Howard SE, Howard TD, Hesdorffer M, et al. Germline BAP1 mutational landscape of asbestos-exposed malignant mesothelioma patients with family history of cancer. Cancer Res 2016;76:206–15. [PubMed: 26719535]
31. Burgie SE, Bingman CA, Soni AB, Phillips GN, Jr., Structural characterization of human Uch37. Proteins 2012;80:649–54. [PubMed: 21953935]
32. Aravind L, Iyer LM. The HARE-HTH and associated domains: novel modules in the coordination of epigenetic DNA and protein modifications. Cell Cycle 2012;11:119–31. [PubMed: 22186017]
33. Dawson MA, Bannister AJ, Gottgens B, Foster SD, Bartke T, Green AR, et al. JAK2 phosphorylates histone H3Y41 and excludes HP1alpha from chromatin. Nature 2009;461:819–22. [PubMed: 19783980]

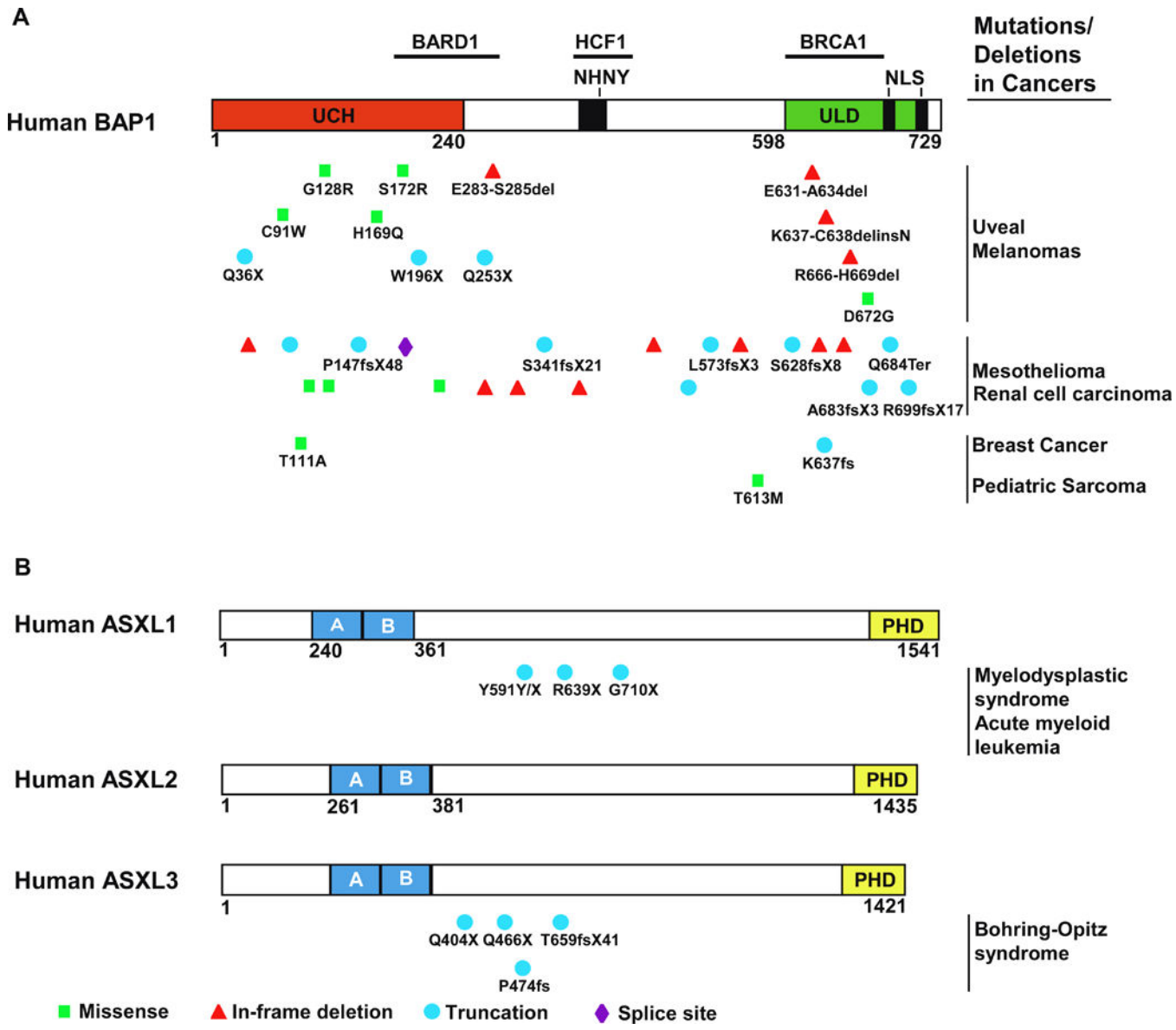

Figure 1.

Domain architecture of human BAP1 and ASXL family members and examples of molecular lesions in human cancers/disorders. (A) Human BAP1 depicting ubiquitin C-terminal hydrolase domain (UCH) (1–240 aa), UCH37-like domain (ULD) (598–729 aa), BARD1 and BRCA1 binding domains, NHNY consensus sequence for interaction with HCF1, and nuclear localization signals (NLS). Also, examples of BAP1 mutations/deletions in uveal melanomas, mesotheliomas, and other cancers. (B) Domain structure of human ASXL family members containing highly conserved AB box and PHD. Examples of ASXL1 mutations in myeloid diseases, and of *ASXL3* in Bohring-Opitz syndrome.

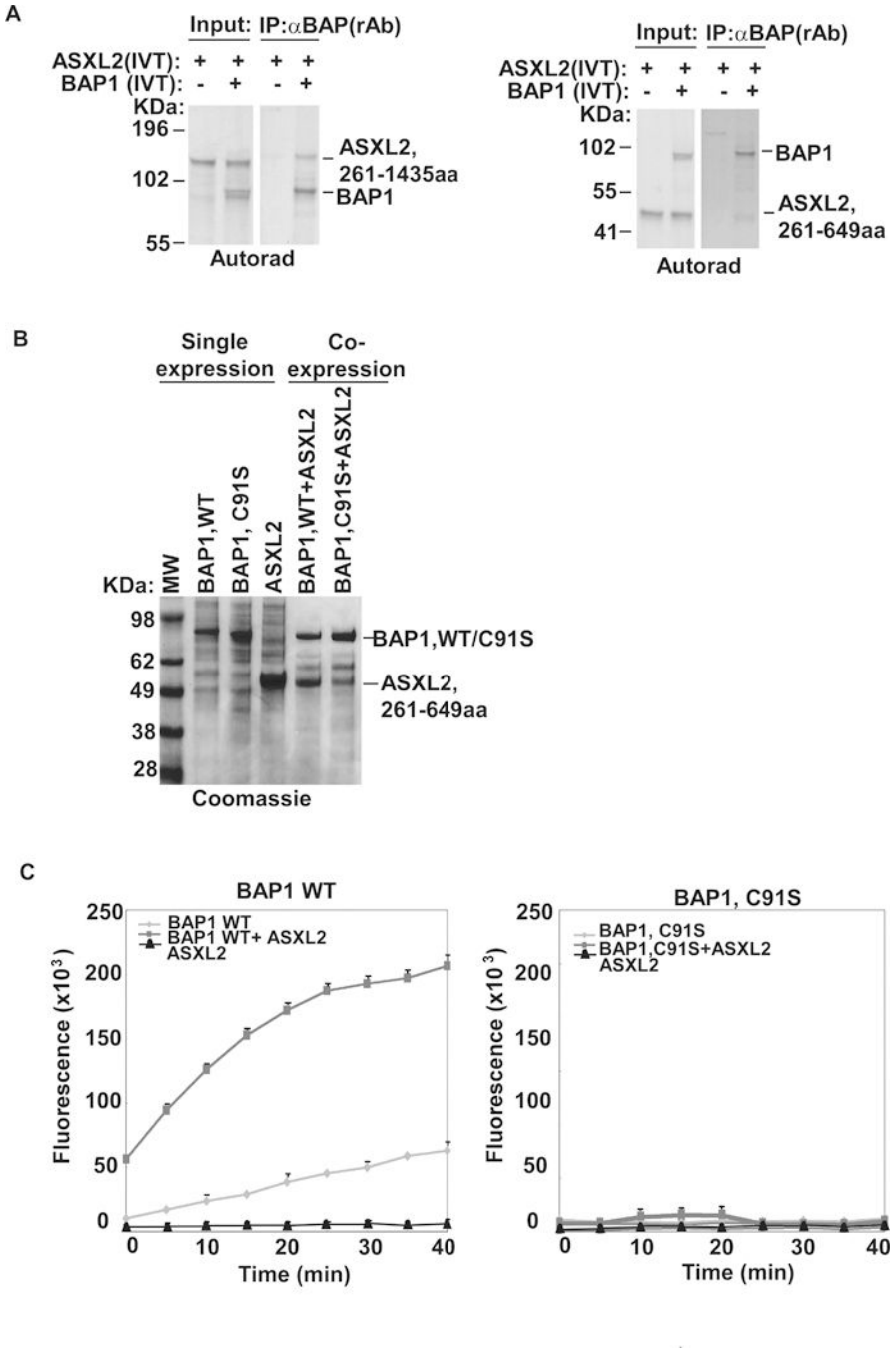

Figure 2.

BAP1 directly interacts with ASXL2, which greatly stimulates BAP1 ubiquitin hydrolase activity. (A) IP performed for ^{35}S-labeled BAP1 and ASXL2 using BAP1 (rAb). (B) BAP1 and ASXL2 produced in Bv by either single-or co-expression. Single-expressed BAP1 WT, BAP1 C91S mutant, and ASXL2 (261–649 aa) proteins were purified with Ni-NTA or ANTI-FLAG M2 Affinity Gel. For co-expression, ASXL2 was co-purified with BAP1 WT or C91S by Ni-NTA resin. Purified proteins were separated on NuPAGE and visualized by

Coomassie staining. (C) Cleavage of Ub-AMC by BAP1 WT/C91S mutant proteins and BAP1-ASXL2 complex. Ub-AMC assay described in Materials and Methods.

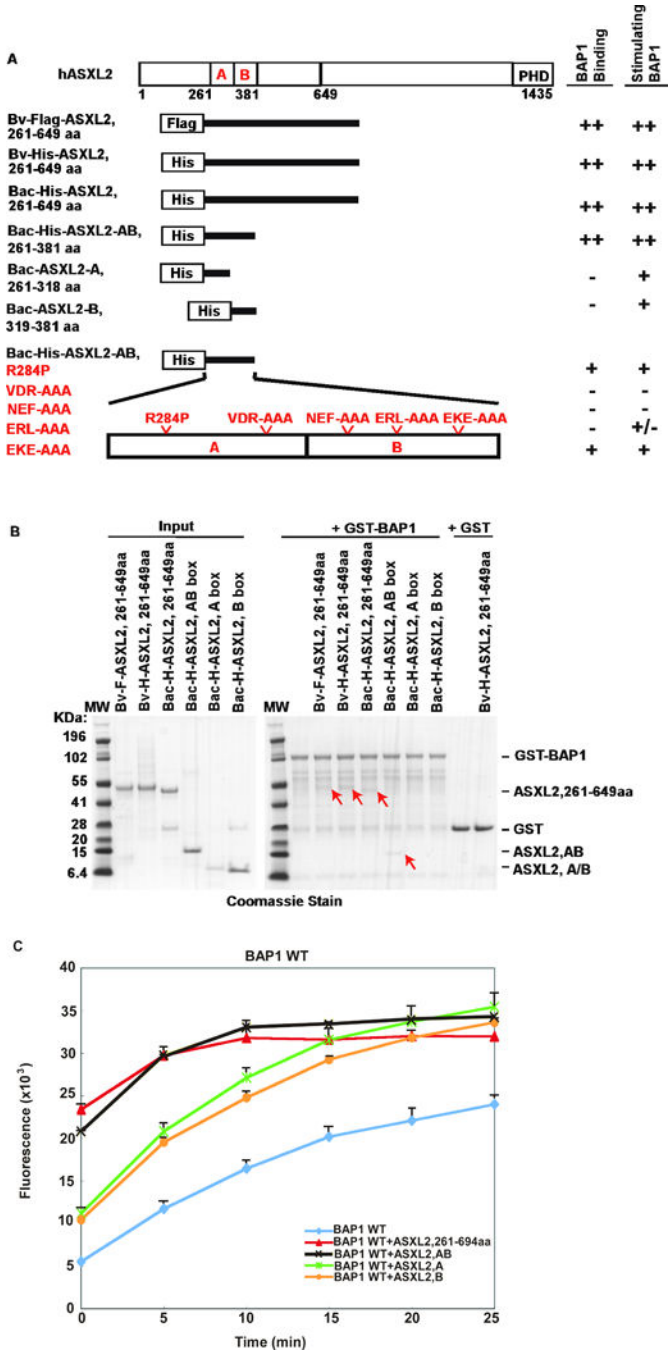

Figure 3.

AB box of ASXL2 is minimal domain for interaction with BAP1 and stimulation of BAP1 ubiquitin hydrolase activity. (A) Summary of minimal domain of ASXL2 interaction with BAP1 and stimulation BAP1 activity. Flag-or His-tagged proteins were produced in Bv or Bac. ++, strongest interaction between ASXL2 and BAP1 and strongest stimulation of BAP1 activity; +, medium interaction and stimulation; –, no interaction/no stimulation. (B) Affinity-purified Flag-or His-tagged ASXL2 truncation proteins separated by NuPAGE (*left*). GST or GST-BAP1 association with truncated ASXL2 proteins. Protein complexes

were separated by NuPAGE (*right*); associated truncated forms of ASXL2 protein with BAP1 indicated by red arrows. (C) Cleavage of Ub-AMC by BAP1 and BAP1-ASXL2 truncation complexes. Ub-AMC assay described in Materials and Methods.

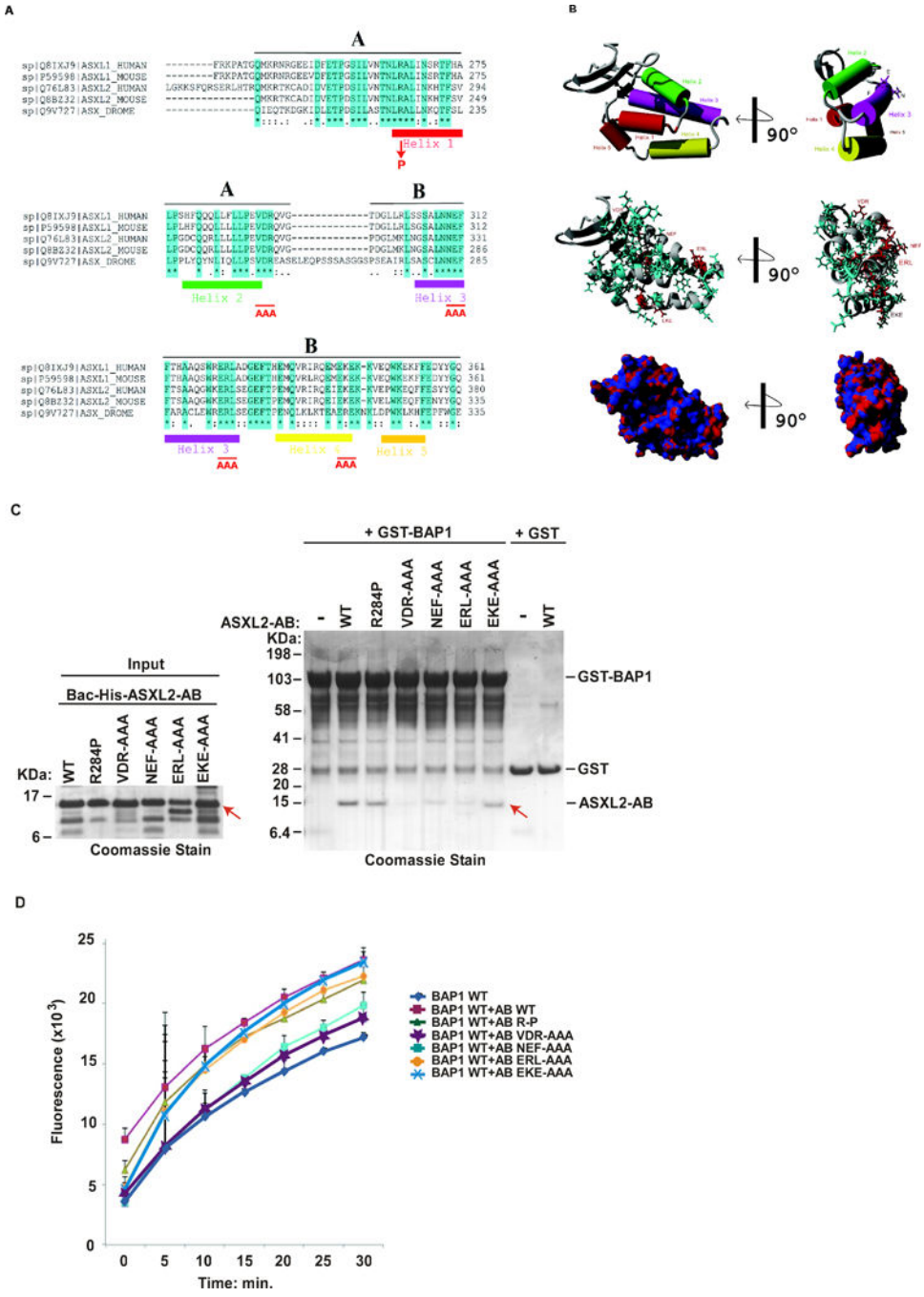

Figure 4.

Highly conserved amino acids in AB box of ASXL are critical for BAP1 interaction and stimulation of BAP1 activity. (A) Sequence alignment of Asx proteins from human, mouse and *Drosophila* (DROME) for ASXH domain showing A and B boxes of domain. Highlighted in cyan are conserved amino acids. Predicted helix locations are marked along with locations of amino acids mutated to P or AAA. (B) Structure prediction for ASXH showing colored helices from A (top), conserved (cyan) and mutated amino acids (red, *middle*), or predicted electrostatic charge (determined with Poisson-Boltzmann Solver) of

domain shown with rotation of 90° on Y-axis for each. (C) His-tagged ASXL2-AB WT and mutant proteins produced from Bac and purified under denaturing conditions, after which proteins were refolded, separated by NuPAGE (*left*). Association of GST or GST-BAP1 with either WT or mutant AB box of ASXL2. Complexes were separated by NuPAGE (*right*); ASXL2-AB box bound to BAP1 indicated by arrows. (D) Cleavage of Ub-AMC by BAP1 and BAP1-ASXL2-AB (WT and mutations) complex. Ub-AMC assay described in Materials and Methods.

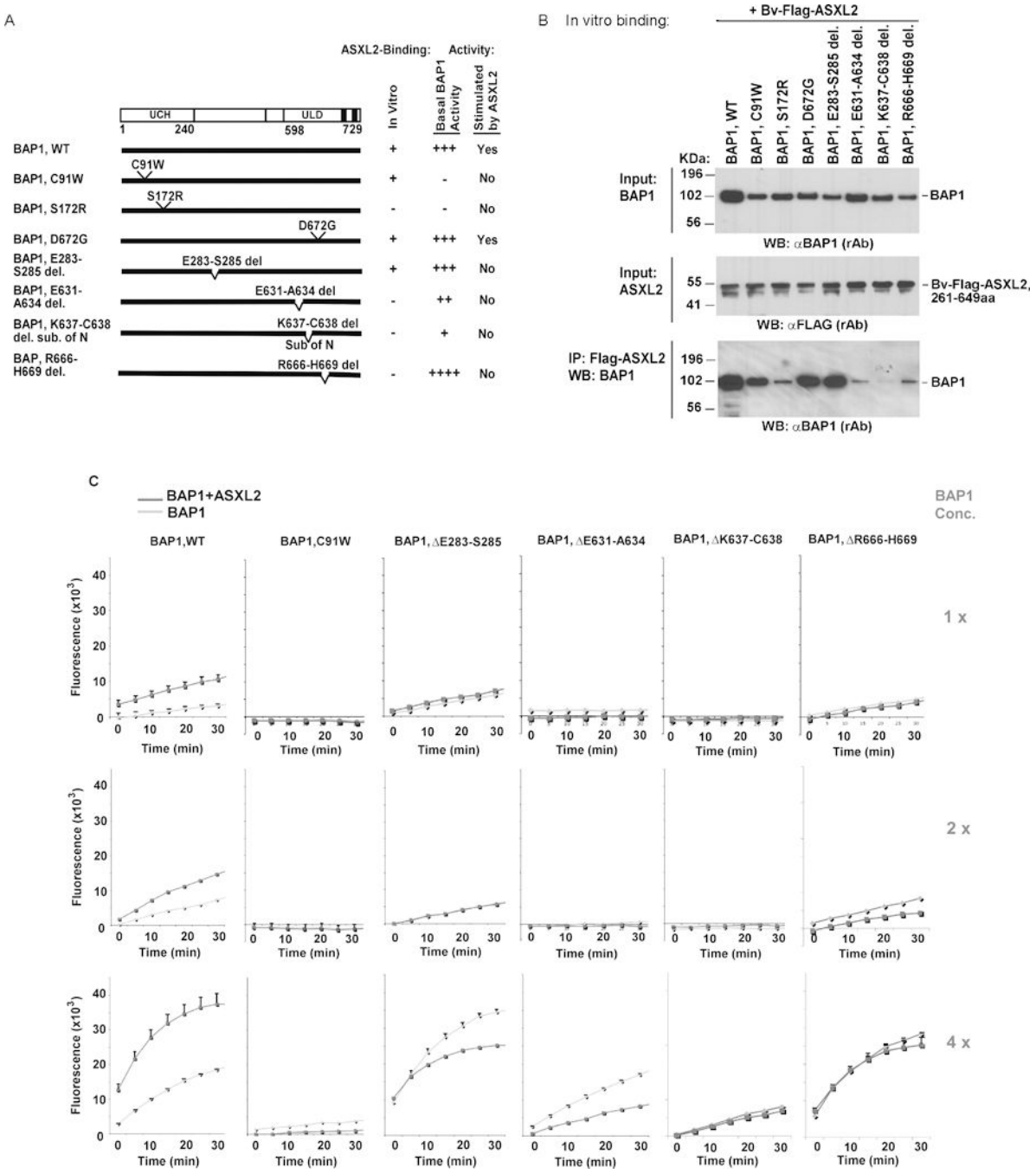

Figure 5.

Cancer-derived mutations/deletions in BAP1-ULD domain abolish ASXL2 association and stimulation activity. (A) Summary of cancer-related mutation/deletions in *BAP1* affecting ASXL2 binding and thereby causing loss of ASXL2 stimulation of BAP1 activity. For ASXL2-binding *in vitro*, + signifies binding of WT or mutant BAP1 to ASXL2 (261–649 aa) *in vitro*, whereas – sign indicates no binding of BAP1 to ASXL2 *in vitro*. For activity, +++ signifies basal BAP1 activity, -indicates kinase dead; *Yes* or *No* indicates whether BAP1 activity is stimulated by ASXL2. (B) Immunoprecipitation for WT and mutant BAP1

associated with ASXL2 bound to αFlag (mAb)-Protein A/G Resin. Complexes were separated by NuPAGE, immunoblotted, and associated proteins detected with αBAP1 (rAb) and αFlag (rAb). (C) Ub-AMC assay is described in Materials and Methods, using different concentrations (1X, 2X, 4X) of indicated protein.

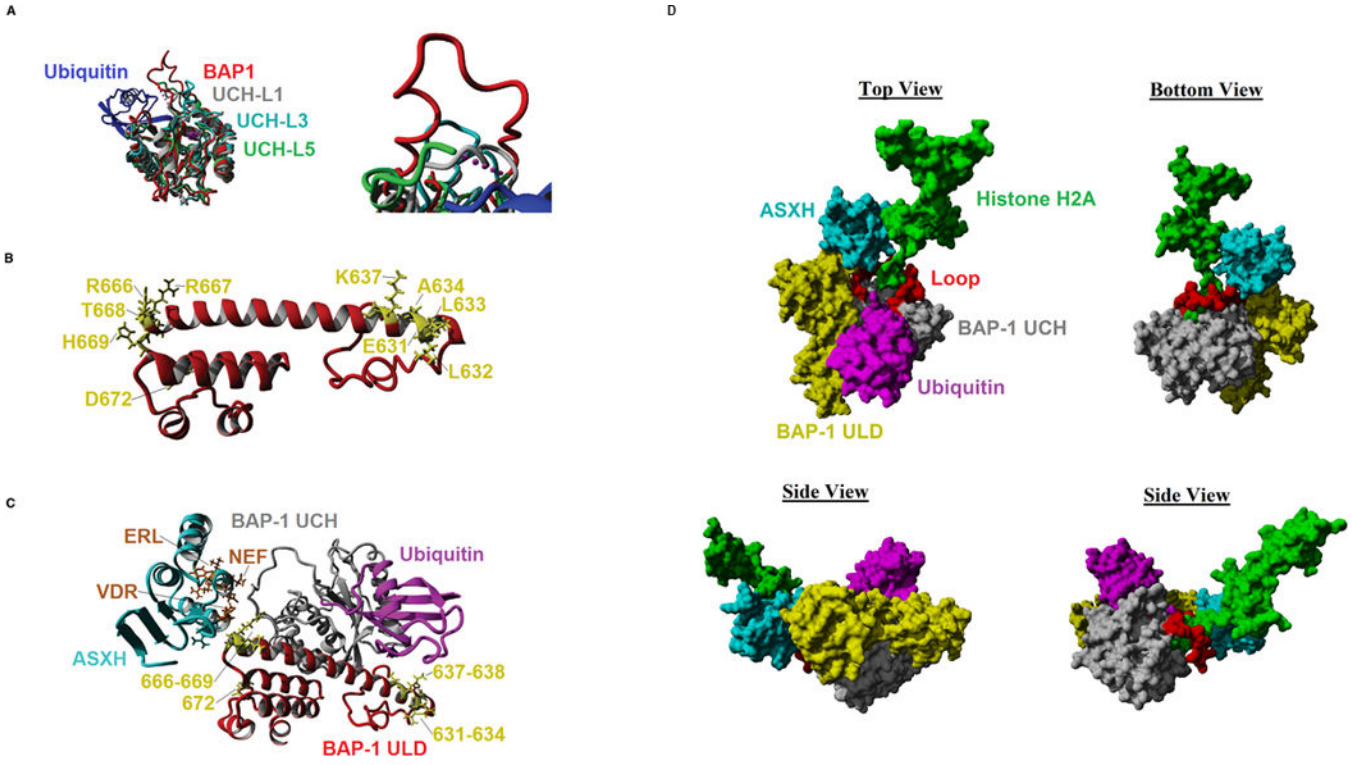

Figure 6.

Molecular modeling of BAP1 and interacting proteins. (A) Alignment of BAP1 (red) model with known UCH domains for UCH-L1 (gray), UCH-L3 (cyan), and UCH-L5 (green) showing homologous folding (*left*), with BAP1 containing the largest loop of all members. Active site Ser indicated in magenta, with binding site for ubiquitin (blue) shown. (B) Model for ULD of BAP1 (red) showing amino acids detected in various cancers (yellow). (C) Model complex of BAP1-UCH (gray) having loop stabilized by ASXH (cyan) and BAP1-ULD (red) allowing for ubiquitin (magenta) to fit into active site. Aberrant amino acids in ULD found in cancer patients shown in yellow, while those identified to decreased interaction between BAP1 and ASXH (VDR, NEF, ERL) depicted in orange. (D) Molecular surface of BAP1 complex allowing for cleavage of histone H2A ubiquitin shown from several views. The combination of BAP1-ULD (yellow) and ASXH (cyan) stabilize loop (red) of BAP1-UCH (gray), allowing for cleavage of ubiquitin (magenta) from histone H2A (green).

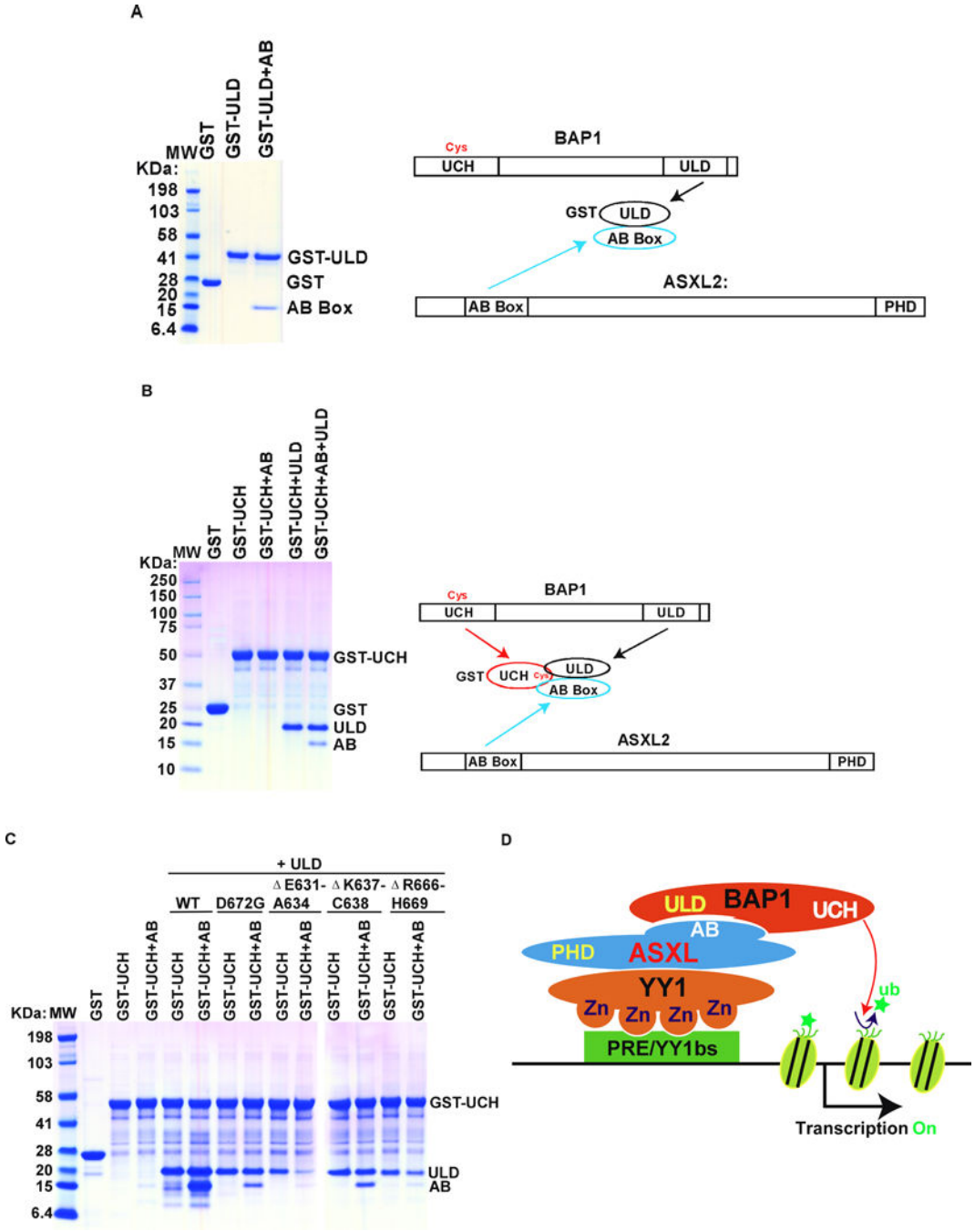

Figure 7.

BAP1-UCH, ULD and ASXL2-AB form ternary stable complex *in vitro*. (A) Binding of ULD of BAP1 and AB box of ASXL2, as demonstrated by GST-ULD pulldown with purified recombinant ASXL2-AB box. (B) Recapitulation of tripartite complex of BAP1-UCH, ULD and ASXL2-AB performed *in vitro*. GST-UCH protein pulldown performed with recombinant BAP1-ULD and ASXL2-AB box. (C) Mutations/deletions corresponding to those seen in cancer patients were introduced to BAP1-ULD proteins. GST-UCH pulldown assay was carried with purified recombinant ULD WT or mutant proteins, and/or

ASXL2-AB. (A-C) Protein complex was separated by NuPAGE. (D) Proposed working model for BAP1/ASXL complex involved in modification of chromatin and regulation of gene transcription.